

Surfactant Mediated Synthesis of Noble Metal Nanoparticles and Their Cytotoxic Effects on Breast Cancer Cells

RAMANJEET KAUR, AVNEET SAINI¹, J. SINGH², P. K. AVTI², V. KUMAR³ AND R. KUMAR*

Department of Physics, ¹Department of Biophysics, Panjab University, Chandigarh 160014, ²Department of Biophysics, Post Graduate Institute of Medical Education and Research (PGIMER), Chandigarh 160012, ³Centre for Medical Physics, Panjab University, Chandigarh 160014, India

Kaur *et al.*: Noble Nanoparticles Cytotoxicity on Cancer Cells

The biomedical applications of the noble metal nanoparticles have been the field of interest, especially in cancer therapy. In this paper, the synthesis of spherical silver and gold nanoparticles and their apoptotic activity against breast cancer cells is reported. The chemicals reduction method is used to synthesize nanoparticles. Two different types of surfactants i.e., citrate and polyvinylpyrrolidone were used as a reducing and capping agent. The synthesized nanoparticles have been characterized using X-ray diffraction, ultraviolet-visible absorption spectroscopy, dynamic light scattering, zeta potential and transmission electron microscopy. The synthesized nanoparticles have crystalline phase with average size in the range of 25-30 nm and possess negative surface charge. *In vitro* studies of nanoparticles against breast cancer cells (MCF-7), were performed. The results show the significant cytotoxicity of nanoparticles against the cancer cell line and found to be mediated by deoxyribonucleic acid damage.

Key words: Breast cancer cell line (MCF-7), deoxyribonucleic acid damage, metal nanoparticles, poly vinyl pyrrolidone, silver nanoparticles, trisodium citrate

Cancer is the largest cause of death worldwide, posing economic and quality-of-life challenges at all levels of society and medical treatment. Chemotherapy is preferable than radiotherapy and surgery in the treatment of cancer because it assures that anticancer medications such as vinblastine, doxorubicin, taxol and cisplatin, among others, reach all disease sites, including micrometastatic lesions^[1,2]. Currently, there are two primary issues with the systematic delivery of cytotoxic drugs during chemotherapy. Firstly, the patient's intrinsic or acquired multidrug resistance and secondly, the dose-limiting toxicity against healthy tissues. In this regard, nanomaterials has become more widely recognized as potentially useful diagnostic and therapeutic tools^[3-5]. Recent advances in synthesis and the potential to rationally modify silver and gold nanoparticle features such as physico-chemical and biological qualities have opened up new avenues for nano-medicine applications^[6,7]. The experimental conditions such as reactants, pH, temperature, order of mixing of reactants, presence of nucleophilic and

electrophilic reagents, nature of stabilizers and even the pace of addition of reducing agents are crucial parameters^[8-10]. These variables influence the advanced nanomaterials size, morphology, stability, colour and physicochemical properties of nanoparticles^[11]. To prevent aggregation in the synthesis and manufacture of metal nanoparticles, natural and synthetic ligands or polymers are commonly utilized as protective/capping agents^[12,13]. The choice of a suitable reducing agent is also critical, since the size, shape and particle size distribution are all influenced by the reducing agent's nature. The introduction of a reducing agent causes the metal precursor to be reduced^[14].

Metal nanoparticles of noble metals, such as silver, gold are particularly well investigated due to their

This is an open access article distributed under the terms of the Creative Commons Attribution-NonCommercial-ShareAlike 3.0 License, which allows others to remix, tweak, and build upon the work non-commercially, as long as the author is credited and the new creations are licensed under the identical terms

Accepted 06 November 2023

Revised 08 February 2023

Received 30 July 2022

Indian J Pharm Sci 2023;85(6):1615-1624

*Address for correspondence

E-mail: rajeshphysicspu@gmail.com

applications in surface enhanced raman scattering and their outstanding properties such as high conductivity, catalytic and antibacterial effect and applications in electronics, catalysis, bio-labeling and other fields^[15-18]. The resonant oscillation of their free electrons in the presence of light causes noble nanomaterials to have substantial optical field enhancements. Noble metal nanoparticles are widely used in optics, imaging, sensing, cosmetics, cancer therapy and medication administration because of their unique features^[19-21]. Metal nanoparticles can be synthesised under simple and moderate conditions. Typical reducing agents including sodium borohydride, hydrazine, sodium citrate, thiols, amino acids and polyols are utilized in the presence of a stabilising layer like Cetyltrimethylammonium Bromide (CTAB), Polyvinyl Alcohol (PVA), cyclodextrin, poly (methylhydrosiloxane) or Polyvinylpyrrolidone (PVP)^[13,14,22-26]. PVP is a type of polymer that is both environmentally friendly and hydrophilic. The use of polymers such as PVP to cap nanoparticles has been recognized as a promising strategy for creating nanoparticles with customizable morphologies and optical properties.

In this study we attempt to synthesize silver and gold nanoparticles using trisodium citrate and PVP as capping agents. The comparative study has been investigated to study the effect of different surfactant capped nanoparticles against the breast cancer cells.

MATERIALS AND METHODS

Materials:

Silver Nitrate (AgNO_3), trisodium citrate ($\text{Na}_3\text{C}_6\text{H}_5\text{O}_7$), PVP, Sodium Borohydride (NaBH_4), Hydrochloroauric acid ($\text{HAuCl}_4 \cdot 3\text{H}_2\text{O}$) were obtained from Sigma Aldrich Chemicals.

Methods:

Tri-sodium citrate capped-silver nanoparticles and gold nanoparticles: For the synthesis of citrate capped silver nanoparticles (AgNPs_c), AgNO_3 (1 mM, 50 ml) was heated and stirred on a hot plate of magnetic stirrer. Then, 1 % tri sodium citrate solution was added drop wise to boiling solution with constant stirring. The absorbance of dark yellow colour indicates, that the formation of AgNPs_c . The tri-sodium citrate act as reducing as well as capping agent^[27].

For synthesis of citrate capped gold nanoparticles (AuNPs_c) in deionized water, a solution of Hydrochloroauric acid ($\text{HAuCl}_4 \cdot 3\text{H}_2\text{O}$) (1 mM, 50 ml) was prepared. Then, 50 ml $\text{HAuCl}_4 \cdot 3\text{H}_2\text{O}$ solution was heated and stirred continuously. When the solution started to boil, aqueous solution of tri-sodium citrate ($\text{C}_6\text{H}_5\text{Na}_3\text{O}_7$) (1 % w/w, 5 ml) was dropped into the boiling solution drop by drop. The solution turned red wine-colored, indicating the formation of AuNPs_c . The tri-sodium citrate acts as reducing and stabilization agent^[27,28]. Fig. 1 depicts a flow chart for the synthesis of AgNPs_c and AuNPs_c .

PVP capped-silver nanoparticles and gold nanoparticles: PVP capped silver nanoparticles ($\text{AgNPs}_{\text{PVP}}$) were synthesized by using NaBH_4 (2 mM, 30 ml) and PVP (0.3 %, 100 μl) which act as reducing and stabilizing agent respectively. An aqueous solution of AgNO_3 was added to ice cold NaBH_4 solution. As soon as the colour of solution changes PVP solution was added. Fig. 1 depicts a flow chart for the synthesis of $\text{AgNPs}_{\text{PVP}}$.

To synthesize $\text{AuNPs}_{\text{PVP}}$, aqueous $\text{HAuCl}_4 \cdot 3\text{H}_2\text{O}$ (1 mM, 50 ml) solution was used as starting solution. The solution was heated at 100° for 30 min to get Au^{3+} ions. These Au^{3+} ions were reduced by adding NaBH_4 (2 mM). To protect the solution against agglomeration, add 100 μl of 1 % PVP at the end of the reaction. Fig. 1 depicts a flow chart for the synthesis of $\text{AuNPs}_{\text{PVP}}$.

Characterization:

Ultraviolet (UV)-Visible absorption spectroscopy: To study optical absorption spectra the samples were scanned in the range of 300-700 nm using LABINDIA UV-3000⁺ spectrometer. The presence of plasmon resonance (SPR) peaked at 420 nm and 520 nm shows the formation of AgNPs and AuNPs respectively.

X-Ray Diffraction: X-Ray diffraction pattern AgNPs and AuNPs were recorded on X' Pert PRO X-Ray diffractometer using $\text{Cu K}\alpha$ (0.15406 nm) radiation. The film was deposited on clean glass slides by drop casting. The scanning speed set at $5^\circ/\text{min}$ and range was selected to $2\theta=35^\circ$ to 80° .

Transmission Electron Microscopy (TEM): The particle shape and size were analyzed by TEM. TEM (Hitachi H-7500, Japan) operating at voltage of 120 kV and equipped with charge-coupled

device camera is used for the ultra-structural determination of synthesized nanoparticles. This instrument has the high resolution of 0.36 nm with 40-120 kV operating voltage and can magnify object up to 600 000 times in high resolution mode. The particle shape and size were analyzed by TEM.

Dynamic light scattering and zeta potential:

The size distribution and zeta potential of AgNPs and AuNPs were studied using Malvern zetasizer (ZEN3600). Dynamic Light Scattering (DLS) was used to examine the particle size distribution of AgNPs_C, AgNPs_{PVP}, AuNPs_C and AgNPs_{PVP}. DLS is used to measure a wide variety of hydrodynamic sizes, ranges from nanometers to a few micrometres.

Cytotoxicity studies:

Cell culture: Breast cancer MCF-7 cells were maintained in continuous culture of Eagles MEM and maintained at 37°, in a humidified atmosphere of 5 % CO₂ supplemented with 10 % FBS. After every 48 h, media was replaced with fresh medium.

Confluent monolayer of MCF-7 cells were detached using trypsin (0.25 %)-ethylenediaminetetraacetic acid (0.02 % in PBS) by spinning at 200 ×g for 2 min followed by washing with serum free medium. Washed pellet were resuspended in 5 ml of complete media Eagle's MEM in T25 flask and incubated at 37° in 5 % CO₂ for further processing.

Cytotoxicity:

After the regular culturing of the cells, approximately 10 000 cells per well were plated into 96-well plate and cultured overnight in CO₂ incubator under humidified conditions. After 24 h cells were treated with various concentrations of AgNPs, AuNPs and standard chemotherapeutic drug palbociclib for different time intervals. After the respective treatment time intervals, cells were treated with 3-[4,5-dimethylthiazol-2-yl]-2,5 diphenyl tetrazolium bromide (MTT) and incubated for 4 h in the CO₂ incubator. Later Dimethyl Sulfoxide (DMSO) was added to dissolve the formazan crystals and absorbance was read at 532 nm in a plate reader for cytotoxicity assessment.

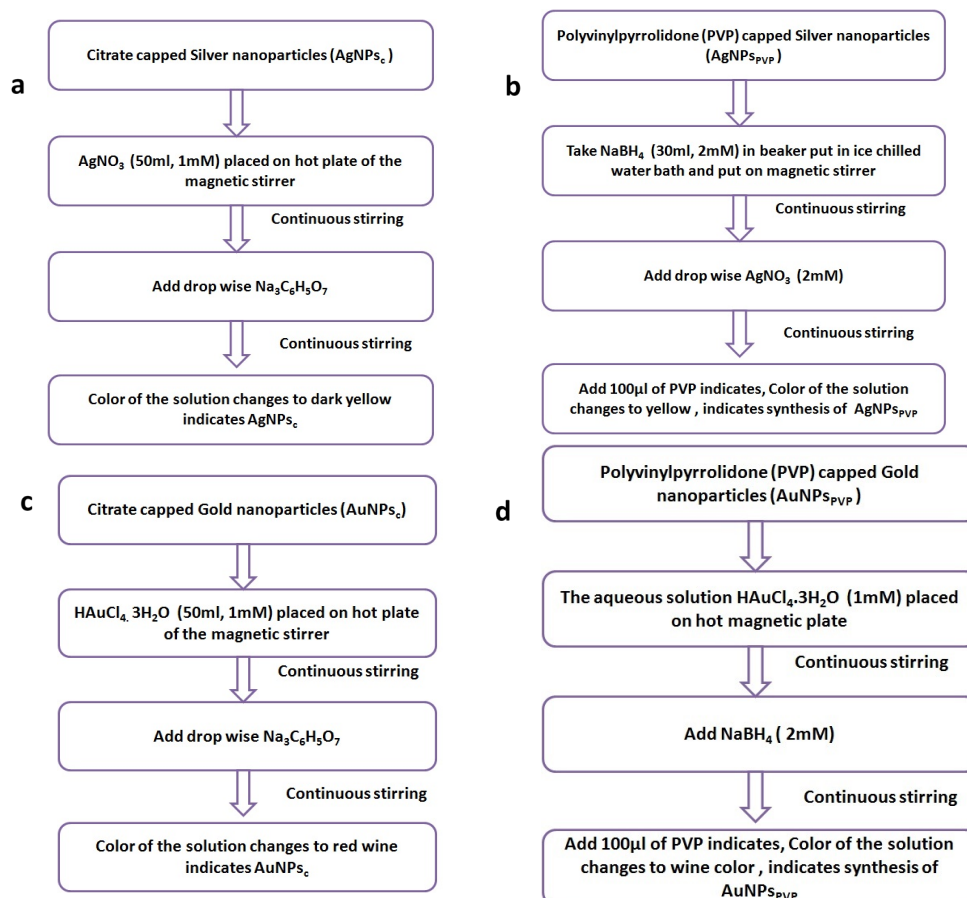


Fig. 1: Flowchart for synthesis of (a) AgNPs_C; (b) AgNPs_{PVP}; (c) AuNPs_C and (d) AuNPs_{PVP}

Structural changes by microscopy:

For studying the metallic nanoparticles-induced structural changes, the treated cells with various concentrations and for different time intervals, the cells were visualized for their morphology under the phase contrast microscope.

Apoptotic activity:

Fluorescence microscopy was performed to assess the AgNPs, AuNPs and palbociclib induced apoptotic activity. To perform these studies, treated the cells with metallic nanoparticles, further were treated with ethidium bromide and acridine orange to evaluate the extent of DNA damage and micronuclei formation.

RESULTS AND DISCUSSION

Fig. 2 shows the UV-visible absorption spectra of silver and gold nanoparticles. The typical SPR peak for spherical AgNPs occurs in the range of 400 nm to 450 nm and for AuNPs range 500-550 nm in the visible part of the electromagnetic spectrum. The absorption spectra shows the SPR peak of AgNPs_C, AuNPs_C, AgNPs_{PVP} and AuNPs_{PVP} at 420 nm, 525 nm, 431 nm and 520 nm respectively. It

can be observed from fig. 2 that SPR peaks of both AgNPs and AuNPs have different points for PVP and citrate capping agents. This is due to different interaction mechanism behaviour of surfactant and nanoparticles. The PVP cationic while citrate is anionic in nature. In the typical chemical reduction method, the tri-sodium citrate act as reducing as well as capping agents for AgNPs_C and AuNPs_C nanoparticles. The atoms are reduced throughout the reaction and subsequently nucleate in tiny clusters, which develop into particles. The precursor to reducing agent ratio, which ultimately governs the amount of atoms obtainable for the reaction, may be changed to control the size and structure of the nanoparticles^[27]. Through an electrostatic stabilization process, the anionic portion of citrate interacts with AgNPs/AuNPs and stabilizes them. PVP is a water-soluble polymer that is broadly utilized in the production of stable silver and gold nanoparticles *via* a steric stabilizing mechanism. PVP contains two extremely active sites for reacting with other molecules, one through the N atom and the other through the -CO atom^[29,30]. PVP functions as a stabilizing agent by interacting with the silver and gold surfaces through the N atom.

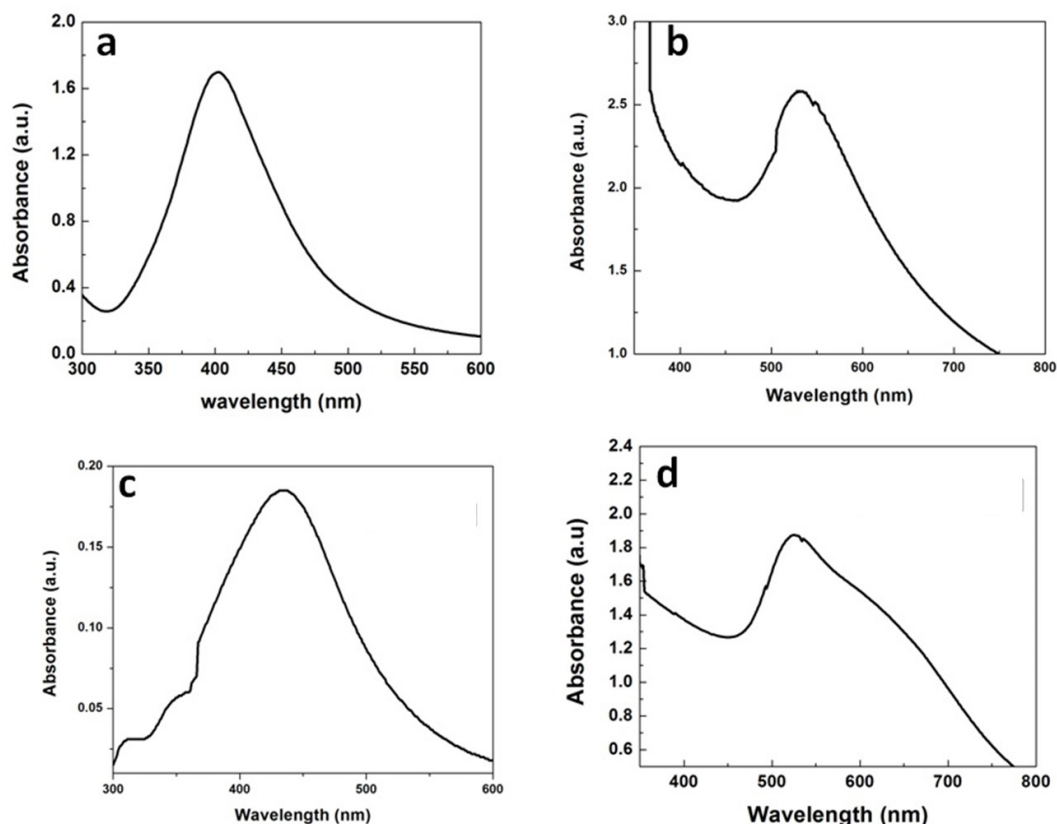


Fig. 2: The UV-Visible absorption spectra of (a) AgNPs_C; (b) AuNPs_C; (c) AgNPs_{PVP} and (d) AuNPs_{PVP} nanoparticles

XRD measurements were used to analyse the crystalline structure of produced AgNPs_C, AgNPs_{PVP}, AuNPs_C and AuNPs_{PVP}. The thin film of sample was prepared by dropcasting on a glass substrate and then diffraction pattern was taken. Fig. 3 shows the XRD pattern of AgNPs_C, AgNPs_{PVP}, AuNPs_C and AuNPs_{PVP}, respectively. The major peaks for AgNPs_C, AgNPs_{PVP}, AuNPs_C and AuNPs_{PVP} were found at 2θ values of 38°, 44.2°, 64.3°, 77.3°, 38.03°, 45.1°, 63.9°, 77.4°; 77.4°; 37.9°, 44.4°, 64.3°, 77.4° and 38.1°, 45.2°, 64.4°, 77.2° respectively correspond to the (111), (200), (220) and (311) crystal planes of face centred cubic structure. These results are similar with standard values of JCPDS file no. 04-0783, 87-0717^[31,32]. The average crystalline size were calculated from Debye Scherer's formula.

$$D = k\lambda / (\beta \cos\theta)$$

Where k Debye Schere's constant, β full width half maxima (FWHM), θ diffraction angle and λ wavelength. The reflection line portion and average crystalline size values are given in Table 1.

Fig. 4 shows the size distribution of AgNPs_C,

AgNPs_{PVP}, AuNPs_C and AgNPs_{PVP}. According to DLS data, synthesized AgNPs and AuNPs with various surfactants were poly-disperse in nature. The Polydispersity Index (PDI) is a measure of the aqueous sample's size distribution or degree of aggregation. Its value in zetasizer software varies from 0 to 1. The samples with a higher PDI value are more polydisperse in nature than those with a lower PDI value, while the samples with a lower PDI value are notably monodisperse. The hydrodynamic average size evaluated for AgNPs_C, AuNPs_C, AgNPs_{PVP} and AuNPs_{PVP} were 38 nm, 40 nm, 44 nm and 43 nm, respectively. It calculates the hydrodynamic radius of Brownian motion particles in aqueous solution by treating them as hard sphere.

Zeta potential gives the charge on the particles, hence Zeta-potential measurements were performed for AgNPs_C, AuNPs_C, AgNPs_{PVP} and AuNPs_{PVP} and shown in fig. 5. The zeta potential for AgNPs_C, AuNPs_C, AgNPs_{PVP} and AuNPs_{PVP} is -20.1 mV, -19.2 mV, -16.9 mV and -12.3 mV, respectively. The negative zeta potential values for the AgNPs_C, AgNPs_{PVP}, AuNPs_C and AgNPs_{PVP} dispersions indicate that the synthesized particles were quite stable for a long period of time.

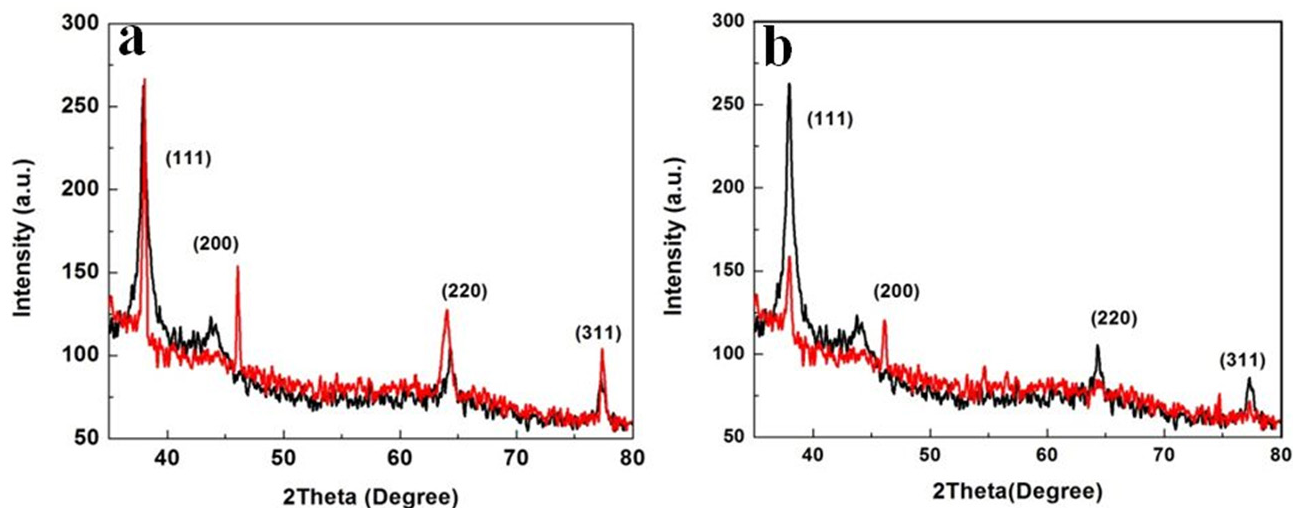


Fig. 3: XRD pattern of (a) AgNPs_C and AgNPs_{PVP} and (b) AuNPs_C and AuNPs_{PVP}, recorded

TABLE 1: THE STRUCTURAL AND HYDRODYNAMICS PARAMERTERS OF SYNTHESIZED NANOPARTICLES

Plane/ material	(111)	(200)	(220)	(311)	Average crystalline size	DLS	Pdl	Zeta potential	TEM
AgNPs _{PVP}	38.03°	45.1°	63.9°	77.4°	~ 20 nm	44 nm	0.39	-16.9 mV	30 nm
AgNPs _C	38°	44.2°	64.3°	77.3°	~10 nm	38 nm	0.64	-20.1 mV	25 nm
AuNPs _C	37.9°	44.4°	64.3°	77.4°	~9 nm	40 nm	0.32	-19.2 mV	25 nm
AuNPs _{PVP}	38.1°	45.2°	64.4°	77.2°	~21 nm	43 nm	0.958	-12.3 mV	31 nm

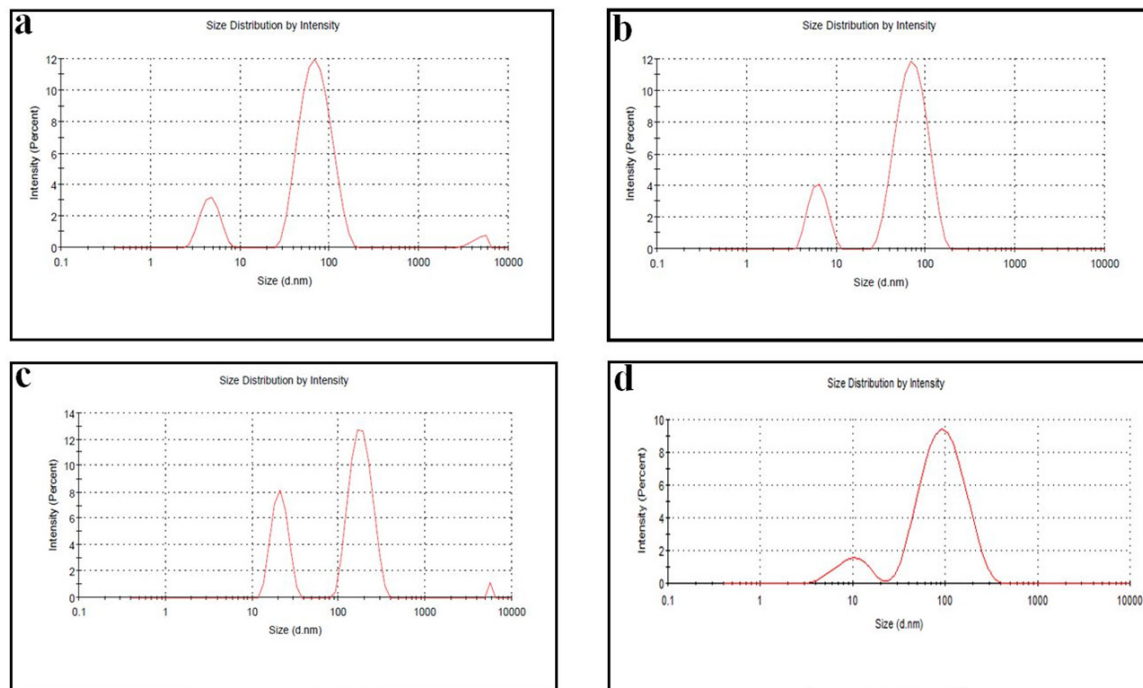


Fig. 4: The size distribution intensity for (a) AgNPs_C, (b) AgNPs_{PVP}, (c) AuNPs_C and (d) AuNPs_{PVP}

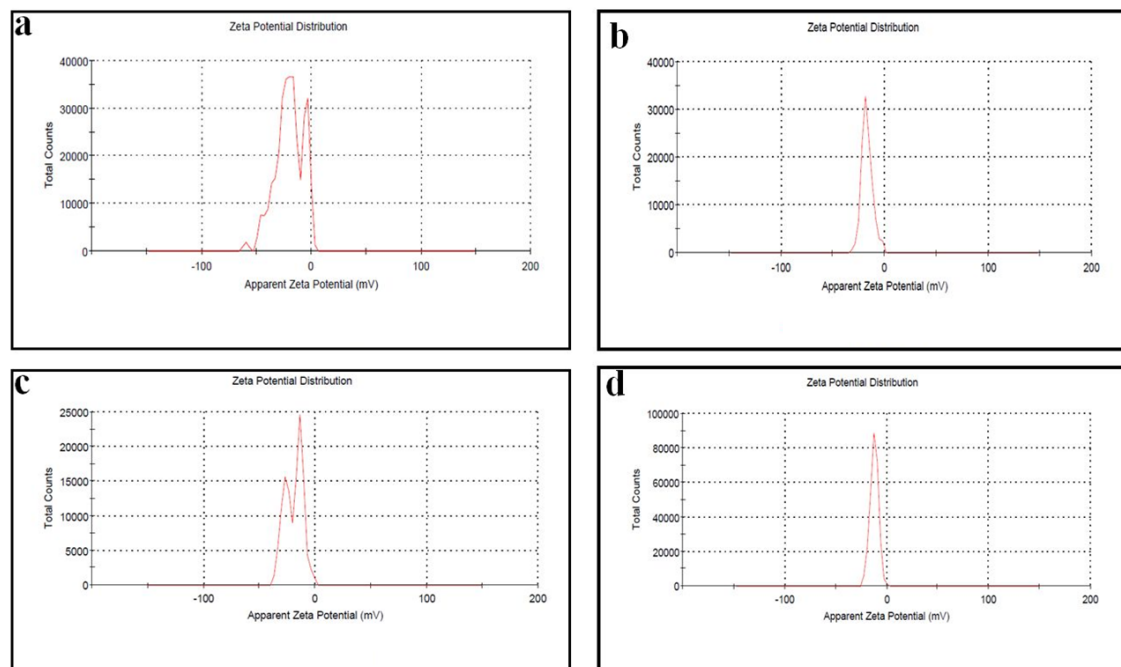


Fig. 5: Zeta potential of (a) AgNPs_C, (b) AgNPs_{PVP}, (c) AuNPs_C and (d) AuNPs_{PVP}

Fig. 6 shows the TEM image of AgNPs_C, AgNPs_{PVP}, AuNPs_C and AuNPs_{PVP}. TEM reveals that the particles were spherical in shape and found to be in the range of 20-35 nm. The average particles size of AgNPs_C, AgNPs_{PVP}, AuNPs_C and AuNPs_{PVP} were 25 nm, 30 nm, 25 nm and 31 nm respectively. The resulting particles are well-distributed and non-agglomerated. The size measured by TEM was

smaller than that obtained by DLS for the identical AgNPs_C, AgNPs_{PVP}, AuNPs_C and AuNPs_{PVP}. The DLS displays the wet and expanded hydrodynamic diameter of AgNPs_C, AgNPs_{PVP}, AuNPs_C and AuNPs_{PVP} suspension, but TEM reveals the dry and shrunk configuration of AgNPs_C, AgNPs_{PVP}, AuNPs_C and AuNPs_{PVP} [33].

The optical microscopy of the various nanoparticles treated for 48 h was performed and it shows that the treatment with AgNPs_C, AgNPs_{PVP}, AuNPs_C, AuNPs_{PVP} is uniform but over longer duration of 48 h the nanoparticles have formed aggregations. The non-aggregated finer respective nanoparticles also shows that these are uniformly spread and being uptaken by the MCF-7 cells. The cells which have uptaken the nanoparticles have shown the structural changes as compared to the normal/control cells where there is no treatment. This can also be seen as in the standard chemotherapeutic drug palbociclib where the cellular structural alterations are significant as compared to the normal cell morphology. To further evaluate the effect of these various nanoparticles on the cell viability MTT assay was performed. Fig. 7 shows the cell viability analysis using MTT assay of breast cancer cells upon treatment with various concentrations of the AgNPs_C, AgNPs_{PVP}, AuNPs_C, AuNPs_{PVP} and standard chemotherapeutic drug at 24 h and 48 h. MTT results shows that there was no significant effect on the cell viability at lower doses as compared to doses at or beyond 20 µl/well (fig. 7a and fig. 7b). However, the cells viability significantly reduced between the ranges 22 %-33 % respectively for the above nanoparticles (fig. 7a). The cells viability further reduced significantly in the dose range 20-40 µl/well with increasing duration (fig. 7b). The cellular viability reduction due to these nanoparticles is comparable to the standard chemotherapeutic drug up to the doses of 20 µl/well but at higher doses the drug palbociclib has significantly reduced further the cell viability as compared to the nanoparticles treated groups. It is also clear from the fig. 7a and fig. 7b that among both the silver nanoparticles, citrate has greater cytotoxic effects as compared to the PVP coated nanoparticles of either metallic nanoparticles. From the optical microscopy and MTT assay we could observe that the nanoparticles had cytotoxic effect on the breast cancer cells and comparable to the standard chemotherapeutic drug up to particular doses. It was also further evaluated to understand the effect of DNA damage, hence, the acridine orange and ethidium bromide studies were undertaken using fluorescence microscopy. It is known that the acridine orange has the ability to bind to the viable cells and ethidium binds to the DNA after damage to the cells. Fig. 8 shows

the fluorescence microscopic images of the DNA damage with various nanoparticles and palbociclib drug treatment. It is seen from these images that the nanoparticles and chemotherapeutic drug treated cells have bright red ethidium bromide staining as compared to the normal cells suggesting that these agents have DNA damaging effect in their cytotoxic behavior (fig. 8). Therefore, it is seen that the silver and gold nanoparticles synthesized from the chemical method using various agents results in the spherical nanoparticles with sizes in the range of 20-35 nm as seen from the TEM and DLS analysis shows strong cytotoxic effect through DNA damage as also seen in and comparable with the chemotherapeutic drug treatment. The nanoparticles in this size range are effectively and easily uptaken by various cell types as seen in many studies^[34]. These nanoparticles having citrate and PVP coatings on their surface have differential aggregation abilities once uptaken by the cells and hence reflect different cytotoxic properties as also seen in this study and compared with the standard chemotherapeutic drug. Therefore, it can be assumed that the gold and silver nanoparticles show potential as nanotherapeutic agents in cancer treatment.

In this study, colloidal silver and gold nanoparticles were synthesized and stabilized with PVP and trisodium citrate. The presence of SPR peaks confirms the formation of spherical nanoparticles in UV-visible absorption spectra. The DLS, TEM, XRD and Zeta potential reveals that the different surfactant nanoparticles morphology were spherical in shape, crystalline in nature, face centered cubic structure and highly stable due to negative zeta potential value. The effect of nanoparticles on the cellular morphology and cytotoxicity studies shows that these nanoparticles are uptaken by the cells and results in the cytotoxic effect and are comparable to the standard chemotherapeutic drug palbociclib. At higher dose of nanoparticles AgNPs_{PVP} show the higher cytotoxicity as compared to AgNPs_C, AuNPs_C, and AuNPs_{PVP}. Further, the cytotoxicity of these nanoparticles also leads to the DNA damage of the breast cancer cells which are also comparable to the chemotherapeutic drug thereby showing the potential as nanotherapeutic agents in cancer treatment.

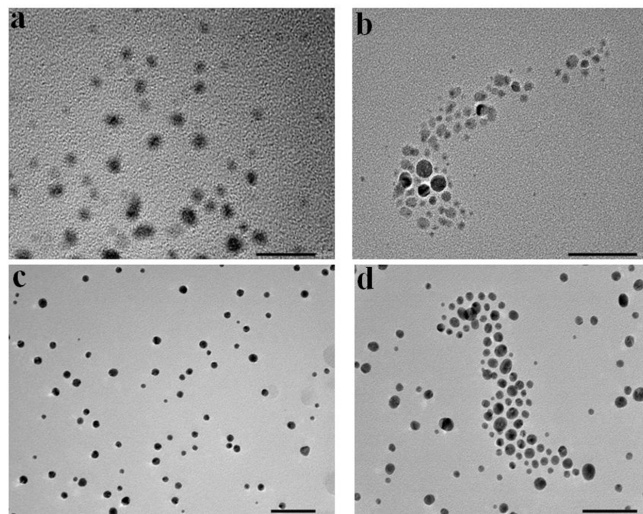


Fig. 6: The TEM micrographs of (a) AgNPs_C; (b) AgNPs_{PVP}; (c) AuNPs_C and (d) AuNPs_{PVP}

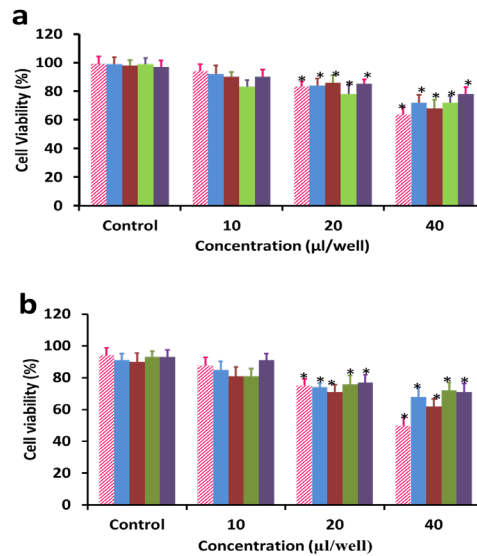


Fig. 7: Cell viability bar graph for MTT assay studies of different surfactant coated silver and gold nanoparticles on breast cancer cells (MCF-7) for 24 h (a) and 48 h (b); On the x-axis the concentration 10, 20 and 40 for palbociclib should be read as 10, 20 and 40 μM respectively

Note: (//): Palbociclib; (■): AgNPs_C; (■): AgNPs_{PVP}; (■): AuNPs_C and (■): AuNPs_{PVP}

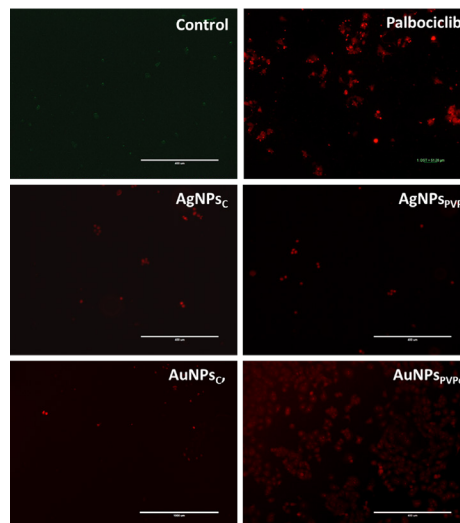


Fig. 8: DNA damage of the Breast cancer (MCF-7) cells changes using fluorescence microscopy (stained with ethidium bromide) at 48 h duration

Acknowledgements:

The authors acknowledge the support received from department of SAIF and CIL, Panjab University, Chandigarh for carrying out TEM characterizations.

Author's contributions:

R. Kaur did the experimentation, data analysis and manuscript writing, A. Saini did data analysis and manuscript editing, data, experimentation, analysis and manuscript writing done by J. Singh. P. K. Avti did conceptualization, analysis and manuscript editing. Vivek Kumar did data analysis and manuscript editing. Rajesh Kumar did idea, conceptualization, analysis and manuscript editing.

Conflict of interests:

The authors declared no conflict of interests.

REFERENCES

- Akram M, Iqbal M, Daniyal M, Khan AU. Awareness and current knowledge of breast cancer. *Biol Res* 2017;50:23-50.
- Klement G, Huang P, Mayer B, Green SK, Man S, Bohlen P, *et al.* Differences in therapeutic indexes of combination metronomic chemotherapy and an anti-VEGFR-2 antibody in multidrug-resistant human breast cancer xenografts. *Clin Cancer Res* 2002;8(1):221-32.
- Singh P, Pandit S, Mokkaapati VR, Garg A, Ravikumar V, Mijakovic I. Gold nanoparticles in diagnostics and therapeutics for human cancer. *Int J Mol Sci* 2018;19(7):1979.
- Sharma H, Mishra PK, Talegaonkar S, Vaidya B. Metal nanoparticles: A theranostic nanotool against cancer. *Drug Discov Today* 2015;20(9):1143-51.
- Chauhan A, Ranjan R, Avti P, Gulbake A. Tailoring the nanoparticles surface for efficient cancer therapeutics delivery. *Int J Appl Pharm* 2020:11-7.
- Jeevanandam J, Barhoum A, Chan YS, Dufresne A, Danquah MK. Review on nanoparticles and nanostructured materials: history, sources, toxicity and regulations. *Beilstein J Nanotechnol* 2018;9(1):1050-74.
- Mody VV, Siwale R, Singh A, Mody HR. Introduction to metallic nanoparticles. *J Pharm Bioallied Sci* 2010;2(4):282.
- Singaravelan R, Alwar SB. Effect of reaction parameters in synthesis, characterisation of electrodeposited zinc nano-hexagons. *J Nanostruct Chem* 2014;4:109-17.
- Suwan T, Khongkhunthian S, Sirithunyalug J, Okonogi S. Effect of rice variety and reaction parameters on synthesis and antibacterial activity of silver nanoparticles. *Drug Discov Ther* 2018;12(5):267-74.
- Mehravani B, Ribeiro AI, Zille A. Gold nanoparticles synthesis and antimicrobial effect on fibrous materials. *Nanomaterials* 2021;11(5):1067.
- Khademi S, Sarkar S, Kharrazi S, Amini SM, Shakeri-Zadeh A, Ay MR, *et al.* Evaluation of size, morphology, concentration, and surface effect of gold nanoparticles on X-ray attenuation in computed tomography. *Phys Med* 2018;45:127-33.
- Ahmed KB, Kalla D, Uppuluri KB, Anbazhagan V. Green synthesis of silver and gold nanoparticles employing levan, a biopolymer from *Acetobacter xylinum* NCIM 2526, as a reducing agent and capping agent. *Carbohydrate Polymer* 2014;112:539-45.
- Kumar A, Das N, Satija NK, Mandrah K, Roy SK, Rayavarapu RG. A novel approach towards synthesis and characterization of non-cytotoxic gold nanoparticles using taurine as capping agent. *Nanomaterials* 2019;10(1):45.
- Dhafer CE, Mezni A, Smiri LS. Surface-enhanced Raman scattering study of Ag-PVP interactions in the biocompatible Ag@PVP nanoparticles. *J Tun Chem Soc* 2017;19:152-7.
- Pal A, Shah S, Devi S. Microwave-assisted synthesis of silver nanoparticles using ethanol as a reducing agent. *Mater Chem Phys* 2009;114(2-3):530-2.
- Oyanedel-Craver VA, Smith JA. Sustainable colloidal-silver-impregnated ceramic filter for point-of-use water treatment. *Environ Sci Technol* 2008;42(3):927-33.
- Moores A, Goettmann F. The plasmon band in noble metal nanoparticles: An introduction to theory and applications. *New J Chem* 2006;30(8):1121-32.
- Austin LA, Mackey MA, Dreaden EC, El-Sayed MA. The optical, photothermal, and facile surface chemical properties of gold and silver nanoparticles in biodiagnostics, therapy, and drug delivery. *Arch Toxicol* 2014;88:1391-417.
- Ibrahim SR, Mohamed GA. Litchi chinensis: Medicinal uses, phytochemistry, and pharmacology. *J Ethnopharmacol* 2015;174:492-513.
- Kshirsagar P, Sangaru SS, Brunetti V, Malvindi MA, Pompa PP. Synthesis of fluorescent metal nanoparticles in aqueous solution by photochemical reduction. *Nanotechnology* 2014;25(4):045601.
- Devadiga A, Shetty KV, Saidutta MB. Timber industry waste-teak (*Tectona grandis* Linn.) leaf extract mediated synthesis of antibacterial silver nanoparticles. *Int Nano Lett* 2015;5:205-14.
- Chahal RP, Mahendia S, Tomar AK, Kumar S. γ -Irradiated PVA/Ag nanocomposite films: Materials for optical applications. *J Alloys Compd* 2012;538:212-9.
- Raza MA, Kanwal Z, Rauf A, Sabri AN, Riaz S, Naseem S. Size- and shape-dependent antibacterial studies of silver nanoparticles synthesized by wet chemical routes. *Nanomaterials* 2016;6(4):74.
- Ng VW, Avti PK, Bedard M, Lam T, Rouleau L, Tardif JC, *et al.* Miktoarm star conjugated multifunctional gold nanoshells: synthesis and an evaluation of biocompatibility and cellular uptake. *J Mater Chem B* 2014;2(37):6334-44.
- Bédard M, Avti PK, Lam T, Rouleau L, Tardif JC, Rhéaume É, *et al.* Conjugation of multivalent ligands to gold nanoshells and designing a dual modality imaging probe. *J Mater Chem B* 2015;3(9):1788-800.
- Avti PK, Maysinger D, Kakkar A. Alkyne-azide "click" chemistry in designing nanocarriers for applications in biology. *Molecules* 2013;18(8):9531-49.
- van Dong P, Ha CH, Binh LT, Kasbohm J. Chemical synthesis and antibacterial activity of novel-shaped silver nanoparticles. *Int Nano Lett* 2012;2:1-9.
- Zhu T, Vasilev K, Kreiter M, Mittler S, Knoll W. Surface modification of citrate-reduced colloidal gold nanoparticles with 2-mercaptosuccinic acid. *Langmuir* 2003;19(22):9518-25.

29. Tanguay JF, Zidar JP, Phillips III HR, Stack RS. Current status of biodegradable stents. *Cardiol Clin* 1994;12(4):699-713.
 30. Agrawal CM, Haas KF, Leopold DA, Clark HG. Evaluation of poly (L-lactic acid) as a material for intravascular polymeric stents. *Biomaterials* 1992;13(3):176-82.
 31. Lei D, Menggen Q, Du L, Te G, Jin T, Zhi Y, Liu J, Fan X. Enhanced field emission from titanium dioxide nanotube arrays decorated with graphene sheets and silver nanoparticles. *Vacuum* 2016;126:29-33.
 32. Khatoon UT, Rao GN, Mohan KM, Ramanaviciene A, Ramanavicius A. Antibacterial and antifungal activity of silver nanospheres synthesized by tri-sodium citrate assisted chemical approach. *Vacuum* 2017;146:259-65.
 33. Wang J, Zhu R, Sun X, Zhu Y, Liu H, Wang SL. Intracellular uptake of etoposide-loaded solid lipid nanoparticles induces an enhancing inhibitory effect on gastric cancer through mitochondria-mediated apoptosis pathway. *Int J Nanomedicine* 2014:3987-98.
 34. Binti Rosli NS, Rahman AA, Aziz AA, Shamsuddin S, Zakaria NS. Effects of the gold nanoparticles (AuNPs) on the proliferation and morphological characteristics of human breast cancer cells (MCF-7) in culture. *Solid State Phenomena* 2017;268:254-8.
-